# A Comprehensive Battery Energy Storage Optimal Sizing Model for Microgrid Applications

Ibrahim Alsaidan, *Student Member, IEEE* Amin Khodaei, *Senior Member, IEEE*, and Wenzhong Gao, *Senior Member, IEEE*

*Abstract*— Microgrids expansion problems with battery energy storage (BES) have gained a great attention in recent years. To ensure reliable, resilient, and cost effective operation of microgrids, the installed BES must be optimally sized. However, critical factors that have a great impact on the accuracy and practicality of the BES sizing results are normally overlooked. These factors include the wide range of characteristics for different technologies, the distributed deployment, the impact of depth of discharge and the number of charging/discharging cycles on the BES degradation, and the coordination of microgrid operation modes. Thus, this paper proposes a comprehensive BES sizing model for microgrid applications which takes these critical factors into account when solving the microgrid expansion problem and accordingly returns the optimal BES size, technology, number, and maximum depth of discharge. The microgrid expansion problem is formulated using mixed integer linear programming. The nonlinear relationship between the BES depth of discharge and lifecycle is linearized using piece wise linearization technique and implemented to model the BES degradation. The proposed model is validated using a test microgrid. The conducted numerical simulation shows that the proposed model is able to determine the optimal BES size, technology, number, and maximum depth of discharge and further enhances the accuracy and practicality of the BES sizing solutions.

*Index Terms*—Battery energy storage, distributed energy resource, microgrid, expansion planning.

### NOMENCLATURE

*Indices*

| | |
|---|---|
| $b$ | Index for bus. |
| $d$ | Index for day. |
| $h$ | Index for hour. |
| $i$ | Index for distributed energy resources. |
| $l$ | Index for lines. |
| $m$ | Index for depth of discharge segments. |
| $s$ | Index for scenarios. |
| $\sim$ | Index for forecasted parameter. |

*Sets*

| | |
|---|---|
| B | Set of BES technologies. |
| K | Set of microgrid buses. |
| L | Set of microgrid distribution lines. |
| N | Set of maximum depth of discharge segments. |
| G | Set of dispatchable units. |
| W | Set of renewable generation units. |
| $\Phi$ | Set of uncertain parameters. |

*Parameters*

| | |
|---|---|
| $BL$ | BES investment budget limit. |
| $CE_i^a, CP_i^a$ | BES annualized energy/power capital cost. |
| $CI_i^a$ | BES annualized installation cost. |
| $CM_i$ | BES annual operating and maintenance cost. |
| $D_{bdh}, CD_{bdh}$ | Total load demand and critical load demand at bus $b$, day $d$, hour $h$. |
| $DR_i, UR_i$ | Ramp down and ramp up rates. |
| $DT_i, UT_i$ | Minimum down and up times. |
| $f_l^{max}$ | Maximum power capacity of distribution lines. |
| $P^{M,max}$ | Maximum power capacity of the line connecting the microgrid to the utility grid. |
| $r$ | Interest rate. |
| $T$ | Project lifetime. |
| $pr_s$ | Probability of islanding scenarios. |
| $v$ | Value of lost load, \$/kWh. |
| $z_{dhs}$ | Microgrid/utility grid connection state. |
| $\alpha_i^{max}, \alpha_i^{min}$ | Maximum and minimum BES energy rating to power rating ratio. |
| $\gamma_{ibm}$ | BES maximum depth of discharge. |
| $\kappa_{im}$ | BES lifecycle. |
| $\rho_{dh}$ | Electricity market price, \$/kWh. |
| $\eta_i$ | BES round trip efficiency. |
| $\mu_{ib}$ | Element of generation-bus incidence matrix (1 if unit $i$ is connected to bus b, 0 otherwise). |
| $\psi_{lb}$ | Element of line-bus incidence matrix (1 if line $l$ is connected to bus b, 0 otherwise). |

*Variables*

| | |
|---|---|
| $C_{ibdhs}$ | Stored energy in the BES at each interval. |
| $C_{ib}^R, P_{ib}^R$ | BES rated energy and rated power. |
| $P_{ibdhs}^{ch}, P_{ibdhs}^{dch}$ | BES charging and discharging power. |

| | |
|---|---|
| $F_i$ | Cost function of the microgrid local DG units. |
| $f_{ldhs}$ | Distribution line power flow. |
| $LS_{bdhs}$ | Load curtailment. |
| $I_{idhs}$ | Commitment state of dispatchable units. |
| $P_{idhs}$ | DER output power. |
| $P^M_{dhs}$ | Power transferred to/from the utility grid. |
| $T^{\text{on}}_{idh}, T^{\text{off}}_{idh}$ | Number of consecutive ON and OFF times. |
| $u_{ibdhs}$ | BES operating state. |
| $x_{ib}$ | BES investment state (1 if installed, 0 otherwise). |
| $w_{ibm}$ | Binary variable that represents the chosen value of the BES maximum depth of discharge for discharge segment $m$ (1 if chosen, 0 otherwise) |
| $\xi_{ibdhs}$ | BES cycle indicator. |
| $\chi^g, \chi^l, \chi^p$ | Auxiliary binary variables for renewable DGs generation, load demand, and electricity price. |

## I. INTRODUCTION

THE urgent need for reducing greenhouse gas emissions, improving the system reliability and power quality, and upgrading the aging transmission and distribution infrastructure, have led to a significant increase in the deployment of distributed energy resources (DERs) in power systems. To ensure reliable operation of power systems under high penetrations of DERs, a comprehensive control method that takes the stochastic nature of DERs into consideration must be implemented, as proposed in [1]. These DERs can also be connected to each other to form a microgrid. The U.S. Department of Energy defines a microgrid as "a group of interconnected loads and distributed energy resources (DERs) with clearly defined electrical boundaries that acts as a single controllable entity with respect to the grid and can connect and disconnect from the grid to enable it to operate in both grid-connected or island modes" [2]. Microgrids can be either AC or DC. These two types of microgrids can also be combined into one hybrid AC/DC microgrids where power conditioning devices should be used to link the AC part and DC part together and to manage their operation [3]. Microgrids are considered as viable enablers of DER integration, and in particular, would facilitate an efficient and reliable integration of emission free renewable distributed generators (DGs) to support the environmental agenda [4]. Renewable DGs, however, produce a variable output power that may impose several challenges to the microgrid operation and control, especially during the islanded operation. Various methods are studied to mitigate the generation intermittency and volatility associated with renewable DGs, including but not limited to demand response [5], generation curtailment [6], cluster of microgrids [7], provisional microgrids [8], and energy storage deployment [9]. The demand response and renewable generation curtailment methods are argued to reduce the microgrid's economic value and/or reliability as they are based on either reducing the available renewable DGs generation or supplied demand (e.g., load shedding or load shifting). In a microgrid cluster, two or more microgrids are connected together to fully utilize their

resources, especially when the connection to the main grid is lost. By optimally managing the local microgrid resources such as dispatchable DGs, renewable DGs, energy storage, and controllable loads, the microgrids operation costs can be significantly reduced [10]. However, such solution raises privacy concerns as microgrid owners would need to exchange information about their microgrid with either other microgrid owners or the system operator. Provisional microgrids significantly facilitate the integration of renewable DGs, however, they require additional investments and control mechanism to ensure a reliable and economic operation. The energy storage, among the rest, is discussed to be the best option for mitigating the challenges imposed by renewable generation and improving microgrid reliability while at the same time reducing the microgrid operation cost. Energy storage can store the excess renewable generation to be utilized when it is beneficial from either an economic perspective (e.g., energy arbitrage) or a technical perspective (e.g., frequency and voltage regulation) [11]. Energy storage applications in microgrids can be further categorized into energy applications and power applications [12]. Energy storage technologies that have high power density and fast response are known to be best suited for power quality and frequency regulation applications. On the other hand, energy storage technologies that have high energy density and long discharging time are well suited for long-term applications including peak shaving and energy arbitrage. Among these technologies, battery energy storage (BES) technology is considered to be the most attractive option due to its technological maturity and ability to provide both sufficient energy and power densities [13].

The BES degradation is greatly related to its operation. How deep the BES is discharged and how many charging/discharging cycles are performed have a significant impact on the BES rate of degradation. The relationship between these operation parameters and the BES lifetime must be taken into account when the BES operation or planning problems are investigated. One of the common approaches used to consider the BES degradation phenomena in the BES operation problem is to add an extra term to the objective function that represents the BES degradation cost in $/kWh (i.e., based on its charged/discharged energy) [14]–[17]. In BES planning problem, however, the Ah-throughput model is normally used to estimate the BES lifetime [18],[19]. In this model, the total delivered energy by the BES during the planning time horizon is computed and compared with the expected Ah (i.e., current-hour) that the BES can deliver during its lifetime, which is typically provided by the manufacturer. This, however, may yield inaccurate estimation of the BES lifetime as the relation between the BES depth of discharge and number of cycles are not taken into consideration.

The topic of energy storage sizing in microgrids for both power and energy applications is extensively investigated in literature. Determining appropriate energy storage size for frequency regulation in an islanded microgrid is presented in [20]–[22]. In these works, the BES is sized to perform frequency regulation services, and thus the economic viability of installing the BES into the microgrid is not investigated. Energy storage sizing for energy applications is studied in [23]–[25]. The optimal energy storage size that minimizes the total planning cost of a grid-connected microgrid is determined in

[23] and [24]. The authors use mixed integer programming (MIP) to formulate the planning problem. In [25] a cost sensitivity analysis for different energy storage technologies and sizes in an islanded microgrid is presented. In [26] and [27], a stochastic programming based model is implemented to study the impact of both BES and demand response on the distribution network expansion problem in the presence of renewable DGs. Optimal sizing for a vanadium redox battery is studied in [28], in which dynamic programming is used to solve the day-ahead unit commitment problem for the microgrid.

It is found that the reviewed publications have either one or more of the following shortfalls: (i) Short time frame (e.g., one day) or static models (i.e., operation snapshots) are used to calculate the optimal BES size, which reduce the accuracy and the practicality of the obtained results; (ii) A single BES technology is considered while ignoring the wide range of available BES with various technical and economical characteristics; (iii) The impact of some decisive factors on the BES lifetime is overlooked, such as the BES depth of discharge, number of charging/discharging cycles, and centralized vs. distributed installations; and (iv) On merely one operation mode (i.e., either grid-connected or islanded) is focused while the required coordination is not taken into account. To overcome these shortfalls, a comprehensive model for BES selection and sizing is proposed in this paper. The proposed model considers upgrading an existing microgrid with BES, i.e., an expansion planning problem, in order to reduce its operation cost and improve its supply reliability. The model can be used by microgrids operators and planners to determine the optimal BES technology, size, and maximum depth of discharge, as well as the required number of BES units in case of a distributed deployment. The problem is formulated using mixed-integer linear programming (MIP).

The rest of the paper is organized as follows: Section II outlines the important and decisive variables (i.e., BES technology, number of units, size, and depth of discharge) in the expansion planning problem. The expansion planning problem is formulated in Section III. Numerical simulations on a test microgrid are provided in Section IV to demonstrate the benefits of the proposed model and to validate its applicability. The discussion on the proposed model and conclusion are provided in Sections V and VI, respectively.

## II. PROBLEM OUTLINE AND VARIABLES

### A. BES Technology

There are a variety of BES technologies with different characteristics such as lead acid, sodium sulphur (NaS), lithium-ion (Li-ion), nickel cadmium (NiCd), and vanadium redox (VR). A comprehensive comparison of BES technologies for power system applications is presented in [29]. The capital cost of the BES is normally composed of power rating cost in $/kW and energy rating cost in $/kWh. Even though these are important factors on selecting the appropriate BES technology to be integrated into the microgrid, they are not the only factors that must be considered. For example, it is true that lead acid battery has the lowest capital cost among other technologies, however, it may not be the best option for performing the applications that require frequent charging/discharging, such as load leveling and energy arbitrage, due to its low lifecycle and

high maintenance cost [30],[31].

### B. Number of BES Units

BES units can be integrated to the microgrid as either aggregated or distributed [32]. Under the aggregated configuration, one large BES is installed, normally close to the utility substation, while under the distributed configuration multiple small-sized BES units are installed in different locations within the microgrid. Distributed BES units provide the microgrid with the required redundancy and flexibility to respond to electricity price variations and ensure the desired load/generation profiles, which will accordingly lead to increase in economic benefits of the installation [33]. With proper control and management, distributed configuration may maximize the installed BES units' lifetime, efficiency, and safety [34]. Moreover, increasing the storage capacity tends to increase the difficulty of BES manufacturing and control [32]. The performance of both aggregated and distributed configurations in wind farm applications is investigated in [35] and [36]. However, these papers do not consider the economic aspect of the problem. The proposed model in this paper has the capability to identify the optimal solution between the distributed and the aggregated configurations and to accordingly determine the number of required BES units under the distributed configuration. This capability stems from the fact that the proposed model takes into account the relationship between the BES depth of discharge and lifecycle.

### C. BES Size

The BES investment cost mainly depends on its size, i.e., the power rating and the energy rating. The oversized BES tends to be economically unattractive while an undersized BES may not render the desired benefits. Fig. 1 depicts the impact of the BES size on the microgrid expansion planning cost [24], where an increase in the size linearly increases the investment cost while reduces the operation cost in a nonlinear fashion. The optimal point is commonly the point that the summation of these two costs is minimum.
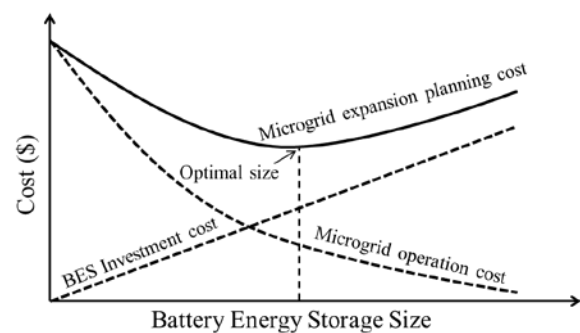


Fig. 1. Microgrid expansion planning cost vs. BES size [24].

### D. BES Depth of Discharge

The BES degradation is mainly caused by two factors: calendric aging and cyclic aging [37]. The former occurs even if the BES is not used and is affected by the BES cells temperature and voltage, while the latter results from using (cycling) the BES and is greatly affected by BES depth of discharge and number of cycles. Disregarding the BES cyclic aging in the expansion planning problem results in an inaccurate economical assessment as the BES might need to be

replaced before the end of the considered project lifetime. Different methods are proposed to estimate the BES lifecycle [38]–[41]. However, it is not uncommon for BES manufacturer to provide the relationship between lifecycle and depth of discharge. This information is normally presented in a curve as the one depicted in Fig. 2. As the depth of discharge increases, the BES lifecycle decreases. Different BES technologies have different lifecycle versus depth of discharge relationships. In lead acid batteries, for example, this relationship tends to exhibit an exponential form whereas in lithium ion batteries a linear relationship is normally observed [38]. The depth of discharge curves are linearized in this paper
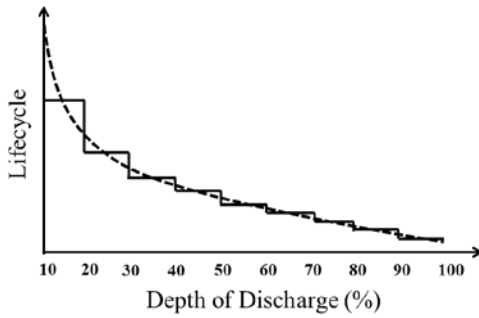


Fig. 2. Linearization of the lifecycle as a function of the depth of discharge.

by using a piecewise linear approximation as depicted in Fig. 2. Increasing the number of segments reduces the approximation error but at the same time increases the computational requirements.

## III. PROBLEM FORMULATION

Expansion planning problems are commonly formulated using MIP [42]–[44]. In MIP, an objective function is typically needed to be either maximized or minimized. This objective function is composed of variables (continuous, integers, or binaries) called decision variables and is solved subject to a set of constraints. If the studied expansion problem consists of nonlinear constraints, these constraints must be linearized first before solving the problem. A commonly used approach to solve MIP problems is branch and bound approach. This approach is based on two processes: 1) bounding process, in which the solution of a relaxed MIP problem (e.g., transforming MIP problem into LP problem by removing integrality restrictions) is found and imposed as lower bound for minimization problems or upper bound for maximization problems; 2) branching process, in which the problem is split into a number of subproblems. A comprehensive discussion on the branch and bound approach is given in Appendix B. Powerful solvers such as CPLEX, Xpress-MP, and SYMPHONEY implement a combination of branch and bound techniques and cutting-plane techniques to accelerate the computation time associated with solving MIP problems, which allows large MIP problems to be solved using personal computers.

Compared with MIP, using nonlinear programming to model the microgrid expansion problem will have two major impacts on the results: (1) solution optimality, as nonlinear programming models may get stuck in a local optimal solution and never reach the global optimal solution, which is not the case in linear programming models; (2) solution time, nonlinear

programming models have higher computation time compared to linear programming models, especially when binary variables are introduced to the problem, which is the case in the proposed microgrid expansion formulation in this paper. In general, it can be said that mixed integer nonlinear programming (MINLP) are hard to be solved and can be numerically intractable [45].

This section discusses in details the objective function and constraints associated with the proposed microgrid expansion model. The objective of the proposed BES optimal selection and sizing problem is to minimize the total expansion planning cost (1) subject to prevailing operational and budget constraints (3)-(22).

$$
\begin{aligned}
Min \sum_{i \in G} \sum_{d} \sum_{h} F_i(P_{idh0}, I_{idh0}) &+ \sum_{d} \sum_{h} \rho_{dh} P_{dh0}^M \\
+ \sum_{s} pr_s \sum_{b \in K} \sum_{d} \sum_{h} LS_{bdhs} v & \\
+ \sum_{i \in B} \sum_{b \in K} \left( P_{ib}^R \left( CP_i^a + CM_i \right) + C_{ib}^R \left( CE_i^a + CI_i^a \right) \right) &
\end{aligned}
\qquad (1)
$$

The first two terms in (1) represent the microgrid operation cost, which is only determined during the microgrid grid-connected mode, i.e., normal operation (as during the islanded mode only the load curtailment is to be minimized). However, if the microgrid is disconnected from the main grid for any reason, the third term in (1) determines the cost associated with failing to supply the microgrid demand (i.e., reliability evaluation). It must be noted that under normal microgrid operation, there will not be any load curtailment as the difference between the microgrid's available generation and demand is picked up by the main grid. This explains the utilization of sub index 0 in (1). That is, index $s$ is used for islanded scenarios which can change from 0 to S. The first scenario (i.e., s=0) represents the grid-connected mode while scenarios s=1,…,S represent various islanded scenarios. The value of lost load (VOLL) is used to quantify the economic loss associated with the unserved energy. The VOLL represents a customer's willingness to pay for reliable electricity service [46]. This value depends on the customer type and location in addition to the outage time and duration. To consider the probability of occurrence of each islanding scenario, $pr_s$ is added as a weighting factor for each scenario. Since there is no load curtailment in the grid-connected mode, the cost of unserved energy for the first scenario (i.e., s=0) will be zero. Due to the expected insignificant changes in the microgrid demand, DGs generation, and electricity price over the planning horizon, one-year historical data are considered in this work. However, if the annual variation of data needs to be included, the proposed model can be easily expanded and solved for longer periods. Another issue to consider is that in the proposed model, the investments are performed in year 1 of the planning horizon, thus enabling an annualized modeling and simulation. This is different from bulk power system planning in which new assets are added in various years, thus requiring multi-year dynamic planning studies.

The BES investment cost is composed of power rating and energy rating capital costs, annual maintenance cost, and installation cost. It is assumed that the power conversion system cost is embedded in the power rating capital cost. The annual maintenance cost is normally given in terms of the BES power

rating whereas the installation cost is given in term of the BES energy rating. Both the BES capital cost and installation cost are annualized using (2)

$$\text{Annualized cost} = \frac{r(1+r)^T}{(1+r)^T - 1} \times \text{One time cost} \qquad (2)$$

The installed BES units are used in the grid-connected mode to increase the economic viability of the microgrid as they store energy at low price periods and generate the stored energy back to the system to be either used by local demand or sold to the utility grid at high price periods. In the islanded mode, however, BES units are used to improve the microgrid reliability by minimizing the curtailed load and the cost of unserved energy. This objective is subject to several operation and technical constraints, associated with the microgrid, dispatchable DGs, and the BES, that must be taken into account as discussed in the following.

### A. Microgrid Constraints

Microgrid's system level constraints include nodal power balance, power exchange with the utility grid, limits on load curtailment and the distribution network power flow (3)-(6).

$$\sum_{i \in \{G,W\}} \mu_{ib}\, P_{idhs} + \sum_{i \in B} \left( P^{\text{ch}}_{ibdhs} + P^{\text{dch}}_{ibdhs} \right) + \sum_{l \in L} \psi_{lb}\, f_{ldhs} + P^{\text{M}}_{dhs}$$
$$\hspace{6cm} (3)$$
$$+ LS_{bdhs} = D_{bdh} \qquad\qquad \forall b \in K, \forall d, \forall h, \forall s$$

$$-P^{\text{M,max}} z_{dhs} \le P^{\text{M}}_{dhs} \le P^{\text{M,max}} z_{dhs} \qquad \forall d, \forall h, \forall s \qquad (4)$$

$$0 \le LS_{bdhs} \le \left( D_{bdh} - CD_{bdh} \right) \qquad \forall b \in K, \forall d, \forall h, \forall s \qquad (5)$$

$$-f^{\max}_{l} \le f_{ldhs} \le f^{\max}_{l} \qquad\qquad \forall l \in L, \forall d, \forall h, \forall s \qquad (6)$$

The nodal power balance (3) ensures that at each bus the power generated form DERs located at that bus plus/minus power flowing to/from the bus equals local demand. If the generation is not sufficient, load would be curtailed to satisfy the power balance. The BES power is positive when discharging and negative when charging. The utility grid power is positive when the power flows from the utility grid to the microgrid, and negative otherwise. Note that the utility grid power is zero at all buses except at the point of common coupling (PCC). It must be noted that the power losses as well as the bus voltage magnitude and angle are ignored in this work. A linear power flow model is needed to be combined with the proposed model in order to solve the full AC power flow without introducing nonlinear equations. Thus, existing power flow models presented in literature (e.g.,[47]–[50]) are not suitable to be used with the proposed model. Equation (4) imposes a maximum limit on the power transferred through the line connecting the microgrid to the utility grid. This equation is modified by including a binary parameter $z$ that indicates the microgrid islanding state. That is, if the value of $z$ is 0, the microgrid is disconnected from the utility grid and operated in the islanded mode; while if it is equal to 1, the microgrid is grid-connected. The value of $z$ is set by the microgrid planner before solving the expansion planning problem and reflects how many hours in a year the microgrid operates in the islanded mode. One of the motivations for microgrid deployment is the continuity of service for critical loads. The critical loads are typically associated with high VOLL so it is not economically advisable to consider them for the load curtailment. Keeping

this in mind, the load curtailment limits can be defined as in (5). The power flow in the microgrid distribution network is limited by the lines capacities (6). A radial distribution network is considered, hence (3) and (6) can efficiently model the power flow in the microgrid distribution network. In the proposed model it is assumed that the microgrid generations and loads are in close proximity, thus active losses are small compared to the power transferred through the microgrid distribution lines and therefore are negligible. In this work, low renewable DGs penetration is assumed. For this reason, the renewable DGs spillage and the ability of using renewable DGs power conditioning units to supply or absorb reactive power is ignored. However, it must be known that under high renewable DGs penetration, these factors must be included in the microgrid expansion problem [51], [52].

### B. Dispatchable DGs Constraints

Dispatchable DGs output power is limited by maximum and minimum capacities (7), variations across two successive intervals, i.e., ramp up and ramp down (8), (9), and minimum up/down time limits (10), (11). Other constraints such as emission and fuel limits can be easily included.

$$P^{\min}_i I_{idh} \le P_{idhs} \le P^{\max}_i I_{idh} \qquad \forall i \in G, \forall d, \forall h, \forall s \qquad (7)$$

$$P_{idhs} - P_{id(h-1)s} \le UR_i \qquad \forall i \in G, \forall d, \forall h, \forall s \qquad (8)$$

$$P_{id(h-1)s} - P_{idhs} \le DR_i \qquad \forall i \in G, \forall d, \forall h, \forall s \qquad (9)$$

$$T^{\text{on}}_{idh} \ge UT_i \left( I_{idh} - I_{id(h-1)} \right) \qquad \forall i \in G, \forall d, \forall h \qquad (10)$$

$$T^{\text{off}}_{idh} \ge DT_i \left( I_{id(h-1)} - I_{idh} \right) \qquad \forall i \in G, \forall d, \forall h \qquad (11)$$

### C. BES Constraints

Although different BES technologies are considered in this paper, the following equations can accurately model their operation.

$$P^{\min}_i x_{ib} \le P^{\text{R}}_{ib} \le P^{\max}_i x_{ib} \qquad \forall i \in B, \forall b \in K \qquad (12)$$

$$\alpha^{\min}_i P^{\text{R}}_{ib} \le C^{\text{R}}_{ib} \le \alpha^{\max}_i P^{\text{R}}_{ib} \qquad \forall i \in B, \forall b \in K \qquad (13)$$

$$0 \le P^{\text{dch}}_{ibdhs} \le P^{\text{R}}_{ib} u_{ibdhs} \qquad \forall i \in B, \forall b \in K, \forall d, \forall h, \forall s \qquad (14)$$

$$-P^{\text{R}}_{ib} \left( 1 - u_{ibdhs} \right) \le P^{\text{ch}}_{ibdhs} \le 0 \quad \forall i \in B, \forall b \in K, \forall d, \forall h, \forall s \qquad (15)$$

$$\xi_{ibdhs} = \left( u_{ibdhs} - u_{ibd(h-1)s} \right) u_{ibdhs}$$
$$\hspace{5cm} (16)$$
$$\forall i \in B, \forall b \in K, \forall d, \forall h, \forall s$$

$$\sum_d \sum_h pr_s \xi_{ibdhs} \le \frac{1}{T} \sum_{m \in N} \kappa_{im} w_{ibm} \qquad \forall i \in B, \forall b \in K, \forall s \qquad (17)$$

$$\sum_{m \in N} w_{ibm} \le x_{ib} \qquad \forall i \in B, \forall b \in K \qquad (18)$$

$$C_{ibdhs} = C_{ibd(h-1)s} - \frac{P^{\text{dch}}_{ibdhs} \tau}{\eta_i} - P^{\text{ch}}_{ibdhs} \tau$$
$$\hspace{5cm} (19)$$
$$\forall i \in B, \forall b \in K, \forall d, \forall h, \forall s$$

$$\left( 1 - \sum_{m \in N} \gamma_{ibm} w_{ibm} \right) C^{\text{R}}_{ib} \le C_{ibdhs} \le C^{\text{R}}_{ib}$$
$$\hspace{5cm} (20)$$
$$\forall i \in B, \forall b \in K, \forall d, \forall h, \forall s$$

The BES power rating is limited by maximum and minimum values (12). For some BES technologies, such as those considered in this paper, the energy rating is correlated to the power rating and cannot be sized independently. A capacity to

power ration ($\alpha$) is used to size the BES capacity and determine the maximum discharge time at rated power (13). If flow batteries such as vanadium redox battery are considered, this constraint can be easily modified to decouple the power rating and the energy rating. The binary variable $x$ is used to indicate the investment state of a BES technology. To consider multi period modeling, this binary should be time dependent. However, in this work the BES is assumed to be installed in the first year. The BES charging/discharging powers are limited by the installed rated power (14), (15), which further impose that the BES power be negative in the charging mode while positive in the discharging mode. The binary variable $u$ is used to represent the BES operating state. The BES can discharge only when $u$ equals 1 and can charge when $u$ equals 0. Each BES technology has a specific lifecycle, which depends on its associated depth of discharge. The BES cycle is typically defined as a complete charge and discharge cycle. Equation (16) is used to determine the BES cycles. The value of $\xi$ will be 1 every time the discharging process is initiated, otherwise it is 0. The summation of the BES cycles over the planning time horizon cannot exceed the determined lifecycle associated with the chosen maximum depth of discharge and desired project lifetime (17). That is, the installed BES does not need to be replaced during the considered project lifetime and therefore the BES replacement cost is not included in (1). The value of $\kappa$ is determined based on the chosen maximum depth of discharge (Fig. 2) in which it is assumed that the curve is divided into N segments. $w$ is a binary variable that represents the chosen maximum depth of discharge segment. It must be noted that the linearization of the BES depth of discharge versus lifecycle curve for each considered BES technology must be performed before solving the optimization problem. That is, the number of cycle associated with each depth of discharge value is entered as an input to the proposed model. Equation (18) ensures that only one maximum depth of discharge value is considered for each installed BES unit. The stored energy in the BES at each time interval equals the stored energy in the preceding interval minus the discharged or charged energy (19). The BES cannot be charged more than its rated energy and cannot be discharged below its minimum value which is defined by the determined maximum depth of discharge (20). It must be noted that the BES can, however, be discharged at any depth of discharge value less than the determined maximum depth of discharge. Finally, the investment cost of the installed BES units is limited by the available budget (21).

$$\sum_{i \in B}\sum_{b \in K}\left(P_{ib}^{R}\left(CP_{i}^{a}+CM_{i}\right)+C_{ib}^{R}\left(CE_{i}^{a}+CI_{i}^{a}\right)\right)\le BL \quad (21)$$

The problem is solved from a microgrid developer perspective, which means that savings in the upstream grid, such as deferred distribution and transmission upgrades as well as benefits of the reduced congestion, are not included. Figure 3 shows a schematic diagram for the proposed BES sizing and selection model.
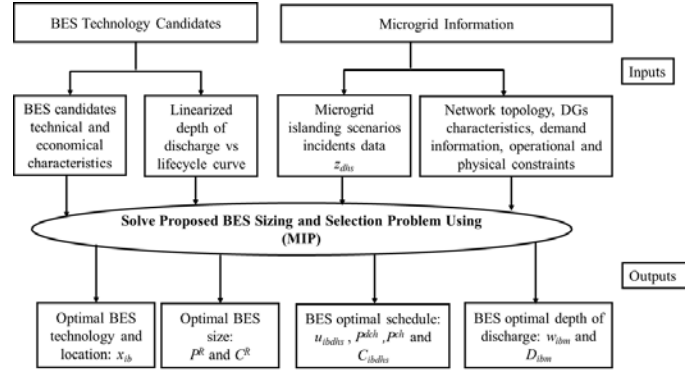


Fig. 3. Schematic diagram for the proposed comprehensive BES sizing model.

### D. Data Uncertainties Consideration

In the presented microgrid expansion planning formulation above, hourly forecasted data for the renewable DGs generation, the load demand, and the electricity price is used. However, forecasting errors may arise as these parameters are affected by uncontrollable factors such as weather conditions, customers' behavior, and congestion or outage incidents. The proposed model can be extended by applying robust optimization method presented in [53] to address the presence of uncertainties in the microgrid expansion problem. Robust optimization determines the worst-case solution by maximizing the minimum value of the objective function (1) over uncertainty set $\Phi$ (i.e., for renewable DG generation, load demand, and electricity price). The objective function in (1) can be rewritten as:

$$\max_{\Phi}\min \sum_{i \in G}\sum_{d}\sum_{h}F_{i}(P_{idh0},I_{idh0})+\sum_{d}\sum_{h}\rho_{dh}P_{dh0}^{M}$$
$$+\sum_{s}pr_{s}\sum_{b \in K}\sum_{d}\sum_{h}LS_{bdhs}v \quad (22)$$
$$+\sum_{i \in B}\sum_{b \in K}\left(P_{ib}^{R}\left(CP_{i}^{a}+CM_{i}\right)+C_{ib}^{R}\left(CE_{i}^{a}+CI_{i}^{a}\right)\right)$$

Uncertain parameters are associated with a nominal value that can be found from the forecast data. These nominal values, however, expand around a range of uncertainty which define an interval within which the uncertain parameter is presumed to lie. Thus, the uncertain parameters can be expressed as:

$$P_{idhs}=\tilde{P}_{idhs}+\overline{P}_{idhs}\overline{\chi}_{idhs}^{g}-\underline{P}_{idhs}\underline{\chi}_{idhs}^{g} \qquad \forall i \in W,\forall d,\forall h,\forall s \quad (23)$$

$$D_{bdh}=\tilde{D}_{bdh}+\overline{D}_{bdh}\overline{\chi}_{bdh}^{l}-\underline{D}_{bdh}\underline{\chi}_{bdh}^{l} \qquad \forall b \in K,\forall d,\forall h \quad (24)$$

$$\tilde{\rho}_{dh}-\underline{\rho}_{dh}\underline{\chi}_{dh}^{p}\le \rho_{bdh}\le \tilde{\rho}_{dh}+\overline{\rho}_{dh}\overline{\chi}_{dh}^{p} \qquad \forall b \in K,\forall d,\forall h \quad (25)$$

where the inserted bars in (23)-(25) represent the upper and lower bounds of each parameter. To ensure only one extreme point is chosen, the following constraints are imposed to the microgrid expansion model at each time interval:

$$\overline{\chi}_{idhs}^{g}+\underline{\chi}_{idhs}^{g}\le 1,\ \overline{\chi}_{bdh}^{l}+\underline{\chi}_{bdh}^{l}\le 1,\ \overline{\chi}_{dh}^{p}+\underline{\chi}_{dh}^{p}\le 1 \quad (26)$$

However, it must be noted that a trade-off between the solution optimality and robustness must be performed when robust optimization method is used. This can be achieved by imposing a higher cap on the maximum number of uncertain parameters that can reach their bounds in the considered planning horizon. This cap is known as the budget of uncertainty [54]. Increasing the budget of uncertainty value will

increase the robustness of the obtained solution at the expense of optimality, and vice versa. If the budget of uncertainty is set to be 0, the problem is solved by ignoring uncertain parameters.

To solve the resulted min-max optimization problem, the duality theory is used to convert the problem into either maximization or minimization problem. For more details about robust optimization formulation and duality theorem, the readers are referred to [53].

## IV. NUMERICAL SIMULATION

A 5-bus microgrid that contains a gas generator, a wind turbine, and a solar photovoltaic unit is used to study the proposed expansion planning model. DGs characteristics and location in the microgrid are given in Table I. The hourly data of renewable DGs generation and local loads are obtained from [55], whereas the hourly data for the electricity market price are taken from [56]. The local load details and location in the microgrid are given in Table II while the microgrid distribution network lines characteristics are given in Table III. The point of common coupling (PCC), which connects the microgrid to the utility grid, is located at bus 1. Four BES technologies are used in the simulation: lead acid, NiCd, Li-ion, and NaS. The characteristics of the BES technologies are borrowed from [29] and shown in Table IV. The power rating of each BES technology is constrained by a maximum value, assumed to be 4 MW in this paper. A minimum discharging time of 1 hour and a maximum discharging time of 5 hours are considered. The BES manufacturers data sheets are used to determine the relationship between the depth of discharge and lifecycle of each BES technology [57]–[60]. Based on the manufacturer data sheet, ten different maximum depth of discharge values are considered for each BES technology (i.e., N=10) through linearization. Increasing N will increase both the accuracy and the computational requirements. Table V indicates the lifecycle of the BES technologies at the considered maximum depth of discharge values. In the Li-ion battery case, the given minimum depth of discharge in the manufacturer data is 50% and no information is given for lower depth of discharge values. One-hour islanded scenarios are implemented to evaluate the reliability of the microgrid under islanded modes (i.e., 24 scenarios for each day), with uniform probability (i.e., $pr$=1/24). The following four cases are studied:

**Case 0:** Microgrid optimal scheduling (i.e., the BES units installation is not included).

**Case 1:** Microgrid expansion planning. In this case, the BES installation to reduce both the microgrid operation cost and the cost of unserved energy is considered.

**Case 2:** This case investigates the impact of ignoring the relationship between the BES depth of discharge and lifecycle on the obtained solution accuracy and practicality.

**Case 3:** The impact of uncertinities associated with renewable DGs generation and load demand on the obtained solution is studied in this case.

TABLE I
DISPATCHABLE GENERATION UNITS CHARACTERISTICS

| Unit | Bus | Type | Cost Coefficient ($/MWh) | Min-Max Capacity (MW) | Min Up/Down Time (hour) |
|------|-----|------|--------------------------|-----------------------|-------------------------|
| 1 | 3 | Gas unit | 90 | 0-7 | 1 |
| 2 | 4 | PV | 0 | 0-1 | - |
| 3 | 4 | Wind | 0 | 0-1.5 | - |

TABLE II
MICROGRID LOCAL DEMAND DETAILS (R: RESIDENTIAL, C: COMMERCIAL)

| Load | Bus | Peak Load (MW) | Critical Load (%) | Load Type | VOLL ($/MWh) |
|------|-----|----------------|-------------------|-----------|--------------|
| 1 | 3 | 6.62 | 60 | C | 50,000 |
| 2 | 5 | 4.41 | 30 | R&C | 50,000 |

TABLE III
DISTRIBUTION LINES CONNECTIONS AND CAPACITIES

| Line | From Bus | To Bus | Capacity (MW) |
|------|----------|--------|---------------|
| 1 | 1 | 2 | 8 |
| 2 | 2 | 3 | 6 |
| 3 | 2 | 4 | 5 |
| 4 | 2 | 5 | 5 |

TABLE IV
BES TECHNOLOGIES CHARACTERISTICS

| Technology | Power Rating Cost ($/kW) | Energy Rating Cost ($/kWh) | Maintenance Cost ($/kW/yr) | Installation Cost ($/kWh) | η (%) |
|------------|--------------------------|----------------------------|----------------------------|---------------------------|-------|
| Lead-acid | 200 | 200 | 50 | 20 | 70 |
| NiCd | 500 | 400 | 20 | 12 | 85 |
| Li-ion | 900 | 600 | - | 3.6 | 98 |
| NaS | 350 | 300 | 80 | 8 | 95 |

TABLE V
BES LIFECYCLES FOR VARIOUS DEPTH OF DISCHARGE VALUES

| Depth of Discharge | Number of Cycles | | | |
|--------------------|------------------|------|--------|-------|
| | Lead acid | NiCd | Li-ion | NaS |
| 10 | 8000 | 7900 | - | 100000 |
| 20 | 2500 | 5800 | - | 60000 |
| 30 | 1500 | 3400 | - | 30000 |
| 40 | 950 | 2000 | - | 15000 |
| 50 | 700 | 1200 | 8000 | 10000 |
| 55 | - | - | 7500 | - |
| 60 | 590 | 900 | 6900 | 9000 |
| 65 | - | - | 6200 | - |
| 70 | 500 | 800 | 5800 | 7000 |
| 75 | - | - | 5000 | - |
| 80 | 450 | 700 | 4500 | 6000 |
| 85 | - | - | 4100 | - |
| 90 | 390 | 600 | 3700 | 5000 |
| 100 | 350 | 500 | 3000 | 4000 |

**Case 0:** To accurately assess the benefits of installing the BES into the microgrid, the pre-expansion case is solved first in order to enable comparisons to the case of BES installation. In this case, the optimization problem is reduced to an optimal scheduling problem in which the objective is to minimize the microgrid operation cost. The total microgrid operation cost is found to be $6,059,253/year. This cost is composed of local units generation cost, power exchanged with main grid cost, and the expected cost of unserved energy. The amount of expected unserved energy in this case is 67.5 MWh/year. This of course would happen only when the microgrid is disconnected from the utility grid and operates in the islanded mode.

**Case 1:** In this case, the BES installation is considered and the proposed mathematical model is used to model the microgrid expansion problem. This case is solved for various project lifetimes. The BES units capital costs and installation costs are annualized according to the considered project lifetime with a 4% interest rate. Moreover, the BES lifecycle is expended over the project lifetime to ensure that once the BES is installed, it does not need to be replaced until the end of the project period. The solution of the proposed model includes the optimal BES technology, or combination of technologies, as well as BES

size, number of BES units, and maximum depth of discharge that minimizes the total microgrid expansion planning cost. In the grid-connected mode, the BES installation reduces the microgrid operation cost by storing energy during low price hours to be used during high price hours toward either supplying local demand (i.e., load shifting) or making economic benefit from selling the stored energy to the utility grid (i.e., energy arbitrage). In the islanded mode, however, the BES reduces the unserved energy, which results in improving the microgrid overall reliability. The obtained results for various project lifetimes are given in Table VI. It is clear from the results that installing the BES is economically justifiable, as the total expansion cost for all the considered project lifetimes is less than the cost of operating the microgrid without BES. Based on the solution of the optimization problem, the BES optimal technology, number of units, size, maximum depth of discharge, as well as the number of annual cycles performed by the BES in the grid-connected mode are given in Table VI.

For the project lifetime of 10 years, a centralized lead acid battery located at bus 2 with the size of 2.905 MW and 5.929 MWh yields the minimum total expansion cost. However, from the BES operation analysis, it is found that the lead acid battery is mostly installed to improve the microgrid reliability under the islanded operation as the number of its cycles in grid-connected operation is low (i.e., 48 cycles). This explains why the lead acid battery is selected as the optimal technology in this case as it is characterized with low capital cost and lifecycle. The lead acid battery is located at bus 2 in order to be available to supply both microgrid demand in the islanded mode of operation which are located at buses 3 and 5. In order for the lead acid battery to perform this number of cycles per year and remains in service for 10 years, its depth of discharge cannot exceed 70%. Installing the lead acid battery is expected to save $7,348/year. However, the big saving is noticed in the islanded operation as the expected unserved energy is reduced by 98.09% compared to Case 1.

When the project lifetime is increased to 15 years, the investment in expensive technologies such as Li-ion and NaS becomes feasible. In this case, it is found that the optimal solution yields when Li-ion and NaS batteries are installed at

$817,125 over the considered expansion timeframe. Both batteries can be discharged up to 80% of their rated energy size. The expected unserved demand in the islanded operation is reduced by 99.68% compared to Case 1.

For a project lifetime of 20 years, the minimum expansion cost is found when two Li-ion batteries are integrated at buses 1 and 4. The optimal size and maximum depth of discharge values for these two BES units are shown in Table VI. The BES installed at bus 4, i.e., where the renewable DGs are located, is used to shift the renewable generation from off-peak periods to the peak periods which will reduce the amount of energy that is needed to be imported from the utility grid during the high price periods and therefore reduce the microgrid operation cost. The BES located at bus 1 is used for energy arbitrage. The expected unserved energy in this case is reduced by 99.26% compared to Case 1.

The BES cycles are computed using equation (16). Fig. 4 shows how the proposed model can accurately compute the BES cycles over the planning horizon. It can be seen from the figure that the summation of the BES discharging cycles ($\xi$) over one week equals to the number of performed cycles over the same period. This enables microgrid planners to take the impact of the number of BES cycles on its lifetime into consideration during the planning stage. Ignoring this impact may require the BES replacement before the expected end of project which imposes an extra cost to the expansion plan.

The other factor that affects the BES lifetime is the depth of discharge, i.e., the amount of energy that can be taken from the BES in each cycle. As discussed in Section III, the number of cycles that the BES can perform before it needs to be replaced is determined by how deep the BES is discharged. Figs. 5-7 depict the SOC for the installed BES units for each considered project lifetime for a sample one week. It must be noted that the determined maximum depth of discharge value puts a cap on how deep the BES can be discharged based on the relationship between the BES depth of discharge and lifecycle. However, the BES can operate with a depth of discharge value that is less than the determined optimal value as can be seen from the state of charge curves (Figs. 6 and 7). The determined maximum depth of discharge value, however, will ensure that the installed

TABLE VI
NUMERICAL SIMULATION RESULTS FOR CASE 1.

| BES Lifetime (years) | Optimal Determined Parameters for the Installed BES | | | | | | Associated Expansion Costs | | | | |
|---|---|---|---|---|---|---|---|---|---|---|---|
| | BES Technology | Bus Number | Power Rating (MW) | Energy Rating (MWh) | Depth of Discharge (%) | Number of Cycles (Cycles/year) | BES Total Investment Cost ($/year) | Local Generation Cost ($/year) | Cost of Power Exchange ($/year) | Expected Cost of Unserved Energy ($/year) | Total Expansion Cost ($/year) |
| 10 | Lead-acid | 2 | 2.905 | 5.929 | 70 | 48 | 377,682 | 834,778 | 1,843,639 | 64,272 | 3,120,371 |
| 15 | Li-ion NaS | 1 3 | 1.461 1.444 | 1.886 1.900 | 80 80 | 300 396 | 432,445 | 834,778 | 1,796,512 | 10,680 | 3,074,416 |
| 20 | Li-ion Li-ion | 1 4 | 2.527 0.401 | 2.865 0.818 | 90 50 | 168 396 | 357,420 | 834,778 | 1,815,893 | 24,960 | 3,033,053 |

buses 1 and 3, respectively. As these technologies can perform a high number of cycles before they reach their end of lifetime, they are used to reduce the microgrid operation cost in the grid-connected mode by purchasing power from the utility grid in low price periods and either use it to supply the demand or sell it to the utility grid in high price period. This saves the microgrid operator $54,475 per year and will sum up to

BES does not need to be replaced during the considered project lifetime which is one of the microgrid planner requirements in this work.

The energy not supplied at each BES lifetime is depicted in Fig. 8. Even though the 15-year lifetime yields the minimum energy not supplied value, it does not yield the optimal solution in terms of microgrid total cost, which is associated with the 20-

year BES lifetime case. To examine the impact of depth of discharge on the overall microgrid expansion cost and to validate the ability of the proposed model to determine the optimal maximum depth of discharge value, the numerical simulation is solved again for a 10-year BES lifetime. Fig. 9 shows the obtained microgrid expansion cost for a variety of depth of discharge values of lead acid battery. It can be seen that the microgrid expansion cost decreases as the depth of discharge increases until it reaches its optimal value found by the proposed model (i.e., 70%) after which the microgrid expansion cost starts to slightly increase again. The change in the microgrid cost is relatively small for depth of discharge values larger than 70%, thus not easily visible in the figure.

**Case 2:** In order to accurately estimate the benefits and the optimal parameters of installed BES, the impact of operation factors such as depth of discharge and number of cycles on the BES lifetime must be included into the microgrid expansion problem. In this section, the importance of considering such impact is investigated. The microgrid expansion planning problem is resolved while ignoring the limit on the BES number of cycles. In other words, the relationship between the BES depth of discharge and lifecycle, which is represented by (17), is omitted from the proposed formulation. A 10-year BES lifetime case is considered. Table VII shows the obtained results for this case. Since the BES operation impact on its lifetime is not included in the model, the optimal BES technology would be the less expensive BES candidate, which is lead acid battery. Moreover, the optimal maximum depth of discharge is found to be 100%. This result, however, is unrealistic as the installed lead acid battery is expected to perform 792 cycles/year. Based on the relationship between the BES depth of discharge and lifecycle, which is given in Table V, the installed lead acid battery must be replaced within the first 5 months from its installation. This shows how important it is to consider the BES operation impact on its lifetime in the microgrid expansion problem in order to enhance the accuracy and practicality of the obtained results.

TABLE VII
NUMERICAL SIMULATION RESULTS FOR CASE 2.

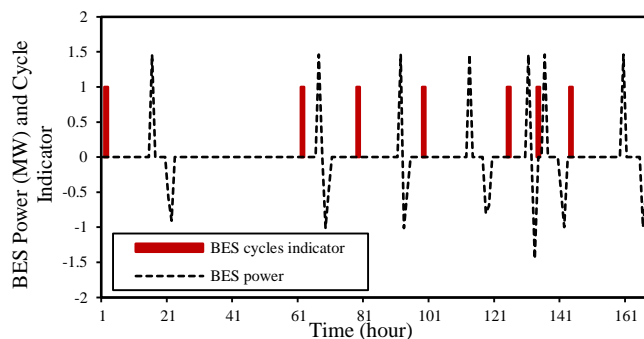| BES Lifetime (years) | Optimal BES Technology | BES Optimal Size (MW/MWh) | Optimal Maximum Depth of Discharge (%) | Number of performed cycles/year | Expected End of Lifetime (months) |
|---|---|---|---|---|---|
| 10 | Lead-acid | 0.823/1.306 | 100 | 792 | 5 |
| | Lead-acid | 2.105/3.341 | 100 | 792 | |



Fig. 4. The Li-ion battery power and cycles for 15-year project lifetime.
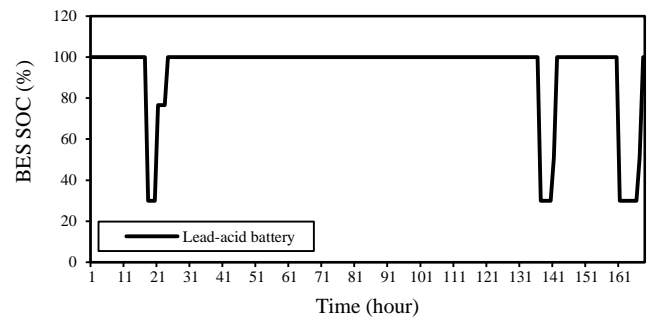


Fig. 5. The installed Lead-acid battery SOC for one sample week (10 years project lifetime).
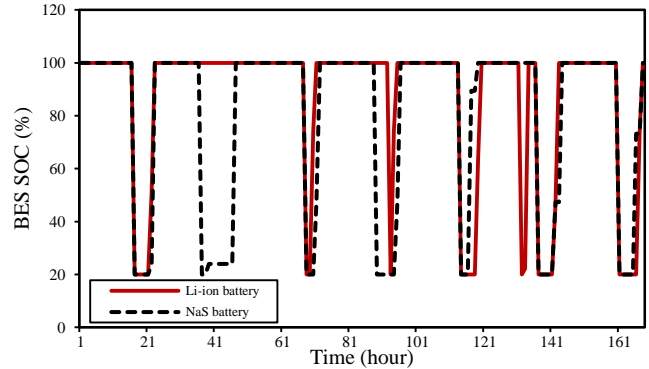


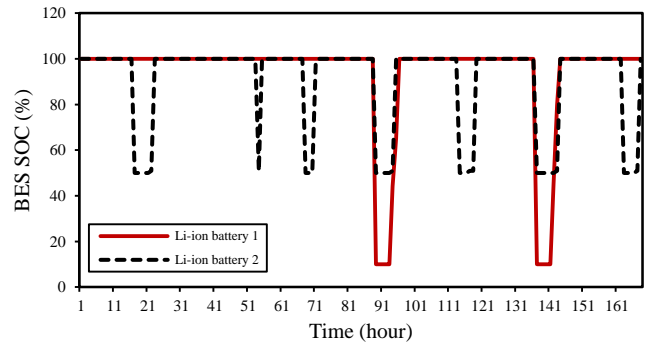Fig. 6. The installed Li-ion battery and NaS battery SOC for one sample week (15 years lifetime).



Fig. 7. The installed Li-ion batteries SOC for one sample week (20 years lifetime).

**Case 3:** In this case, the forecast errors in renewable DG generation and load demand impacts on the obtained solution are investigated. The worst-case scenario occurs when a reduction in renewable DG generation and increase in load demand compared to the forecasted data take place. Thus, -20% forecast errors in renewable DGs generation and +10% forecast errors in load demand are considered. These forecast
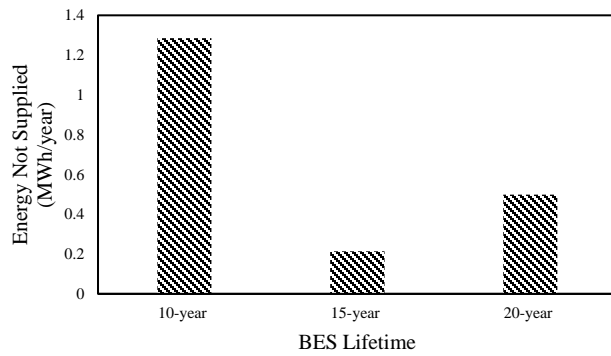
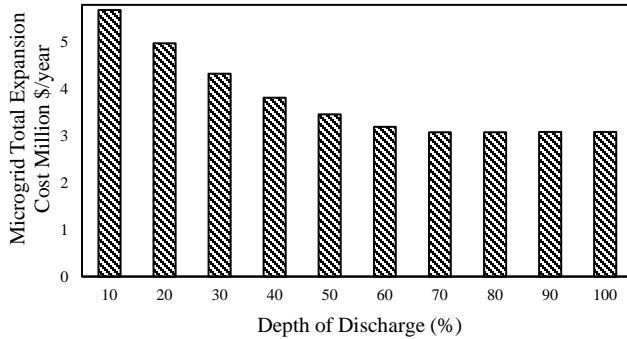Fig. 8. Energy not supplied for the considered BES lifetime.



Fig. 9. Microgrid total expansion cost for different depth of discharge value (10-year BES lifetime case).

errors are assumed to happen for 1000 hours/year. Increasing or decreasing the number of hours per year at which the uncertainties are considered leads to more conservative or aggressive solution against data uncertainties. In the conservative solution, the obtained results are more robust against uncertainties but at the same time higher microgrid expansion cost is expected. On the other hand, the aggressive solution yields less robust results against uncertainties with lower microgrid expansion total cost compared to the conservative solution. The 1000 hours/year used in this simulation can be considered as a moderate solution. The 10-year BES lifetime case is resolved here using the proposed model with the consideration of uncertainties. From the numerical simulation results, it is found that when the uncertainties associated with renewable DG generation and load demand are taken into consideration, the microgrid total expansion cost increases to become $3,368,200/year. Moreover, expensive BES technologies, which are characterized with high lifecycle such as NaS battery become economically feasible. The optimally determined parameters of the installed BES units are given in Table VIII. The reason behind installing NiCd and NaS batteries instead of lead acid battery, which is found to be the optimal BES technology in Case 1, is that considering the uncertainties in the microgrid expansion problem requires the installed BES to be used more frequently in order to overcome the rapid change in the renewable DGs generation and the load demand, especially during islanding operation. Thus, BES technology with high lifecycle is needed in such case. A summary of the studied cases' advantages and disadvantages are shown in Table IX.

TABLE VIII
NUMERICAL SIMULATION RESULTS FOR CASE 3.

| BES Lifetime (years) | Optimal BES Technology | BES Optimal Size (MW/MWh) | Optimal Maximum Depth of Discharge (%) | Number of performed cycles/year |
|---|---|---|---|---|
| 10 | NiCd | 2.483/2.922 | 100 | 48 |
| | NaS | 1.510/1.987 | 50 | 600 |

TABLE IX
STUDIED CASES SUMMARY

| Case | Pros | Cons |
|---|---|---|
| 0 | • No BES investment cost as the BES is not installed in this case. | • High microgrid operation cost and low reliability, especially during islanded operation. |
| 1 | • Improve the microgrid reliability by supplying demand during islanded incidents.<br>• Reduce operation cost by using BES to perform energy arbitrage application.<br>• Impact of BES depth of discharge on its lifetime is considered. | • Stochastic nature of renewable DGs generation and load demand is not included in the expansion problem. |
| 2 | • Microgrid total expansion cost is reduced as the impact of BES depth of discharge on its lifetime is ignored. | • Unrealistic results are obtained and thus the BES will need to be replaced before the end of the desired project lifetime. |
| 3 | • The obtained result is robust against renewable generation and load demand uncertainties. | • High microgrid total expansion cost.<br>• The optimality of the obtained solution might be impacted. |

General algebraic modeling system (GAMS) is used to solve the optimization problem in the studied cases. The problem is implemented on a 2.4-GHz personal computer using CPLEX 11.0. The obtained solution is found within a 0.05% gap of the optimal solution; hence it provides a near-optimal solution. The gap is adjusted using the built-in functionalities of CPLEX in which in each iteration an upper bound and a lower bound of the current solution are calculated and the relative difference is considered as an optimality gap. It is worth noting that in the long-term planning problem it is not always possible to achieve the optimal solution due to the complexity of the problem and the large number of binary and continuous variables. The computation time, however, depends on the considered case, the number of islanding scenarios, and the optimality gap among other factors. For the first case (i.e., the microgrid scheduling problem without the BES installation) the problem is solved within seconds. When the BES installation is included to the problem, the problem is solved within multiple hours. The highest computational time is slightly less than 18 hours. However, as the problem in hand is an expansion planning problem, it is solved offline where the computation time is not as important as in operation problems.

## V. DISCUSSION

Based on the reviewed literature and the obtained results from the conducted numerical simulations, the following is concluded:

- Installing the BES into the studied microgrid reduced the operation cost of the microgrid while at the same time improved the system reliability by reducing the amount of unserved energy during islanded operation.
- The proposed model in this paper was able to accurately determine the optimal BES size,

technology, units' quantity, and maximum depth of discharge that minimizes the total microgrid expansion planning cost while considering the microgrid islanded operation and the BES degradation.

- The obtained results showed that ignoring the impact of BES operation on its lifetime results in an unrealistic solution in which the installed BES might end up costing much more than what was determined before installing the BES.
- Considering the renewable generation and load demand uncertainties impacted the obtained optimal solution as larger BES size and higher number of cycles are required. Thus, robust solution against parameter uncertainties can be achieved with the expense of higher BES investment cost.

## VI. CONCLUSION

A comprehensive BES optimal sizing solution for microgrid applications was proposed in this paper. Critical factors such as the wide range of characteristics for different technologies, the distributed deployment, the impact of depth of discharge and the number of charging/discharging cycles on the BES degradation, and the coordination of microgrid operation modes are taken into consideration in the proposed model. A BES degradation model that is based on the relationship between the BES depth of discharge and lifecycle was implemented in the proposed BES sizing model to accurately estimate the impact of BES operation on its lifetime. Moreover, a set of islanded scenarios was included in the model to determine the microgrid reliability when it operates in the islanded mode. Numerical simulations performed on a test microgrid validated the effectiveness of the proposed model. Robust optimization approach was employed to address the uncertainties associated with renewable DGs generation and load demand.

A follow-on work of this research will focus on studying the impact of using the BES for multiple applications in the BES optimal sizing. In order to study the ability of the BES to perform some applications such as voltage support, congestion relief, and system upgrade deferral, a linear power flow model that can be used to calculate the voltage magnitude and angle at each bus and the active and reactive power flow must be developed.

## APPENDIX A

Linearization of bilinear terms: if variable $y$ is equal to the multiplication of continuous variable $\beta$ and $k$ binary variables $\delta_1, \delta_2, \delta_3, ..., \delta_k$ such as illustrated in (A1), it can be described by $2(k+1)$ constraints as shown in (A2)-(A3). $M$ is a large positive constant.

$$y = \beta \, \delta_1 \delta_2 \delta_3 ... \delta_k \tag{A1}$$

$$\beta - \sum_{j=1}^{k} M\left(1 - \delta_j\right) \le y \le \beta + \sum_{j=1}^{k} M\left(1 - \delta_j\right) \tag{A2}$$

$$-M\delta_j \le y \le M\delta_j \qquad \forall j \in (1,2,3,...,k) \tag{A3}$$

If at least one binary variable is zero, according to (A3), $y$ would be zero, and (A2) would be relaxed. If all binary variables are one, all $k$ constraints in (A3) would be relaxed, and according

to (A2), $y$ would be equal to $\beta$. Therefore, the equation is linearized, and the results of the constraints defined in (A2)-(A3) conform to the original equation in (A1).
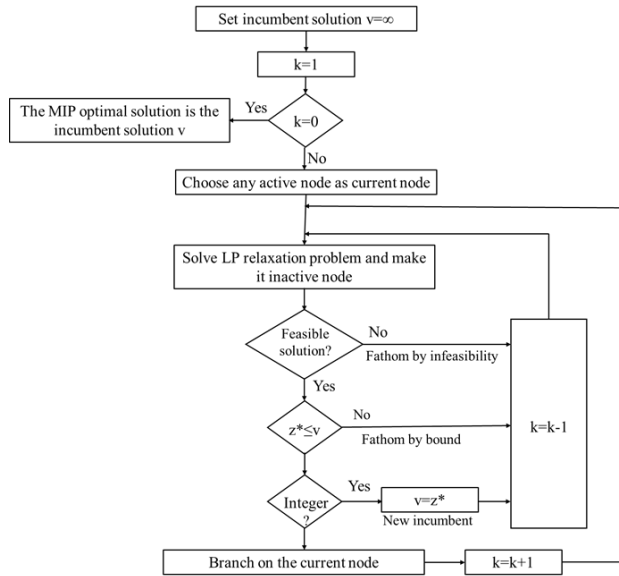
## APPENDIX B

A commonly used approach to solve MIP problems, such as the one presented in this paper, is the branch and bound approach. Before explaining how this approach works, a concept of MIP relaxation must be introduced. A relaxed MIP problem can be defined based on the following two characteristics [54]:

1) Any solution to the original MIP problem is also a feasible solution to the relaxed problem.

2) The objective function value associated with the original MIP solution is larger than or equal to the objective function value associated with the relaxed problem solution.

A typical relaxed MIP problem is its corresponding LP problem, which can be found by removing any integrality constraints in the original MIP problem. To this end, solving the corresponding LP problem will yield one of three possible cases: infeasible solution, feasible solution that satisfies the original MIP integrality constraints, or feasible solution that does not satisfy the original MIP problem integrality constraints. If there is no solution to the LP problem, then the problem is said to be infeasible and some of the constraints must be relaxed or the problem should be reformulated. In case of a feasible solution, if the obtained LP solution happens to satisfy the original MIP integrality constraints, then the LP solution is the optimal solution for the original MIP problem. However, such optimistic case does not happen often and the LP solution normally tends not to comply with the MIP integrality constraints. In this case, the LP problem is divided into two sub-problems. This process is known as branching as the LP problem is branched into sub-problems. These sub-problems are solved and the obtained solutions are compared with each other. If the solutions of both sub-problems satisfy the integrality conditions, they must be compared and the sub-problem solution that is associated with smaller objective function value for minimization problem or larger objective function value for maximization problem is selected as the optimal solution. If only one sub-problem solution satisfies the MIP integrality conditions, then this solution is saved as incumbent solution (i.e., the optimal solution if no better solution is found) while the branching process is continued on the second sub-problem searching for a better solution that satisfies the MIP integrality conditions. The branching and bounding steps are shown in the following figure.

This article has been accepted for publication in a future issue of this journal, but has not been fully edited. Content may change prior to final publication. Citation information: DOI 10.1109/TPWRS.2017.2769639, IEEE Transactions on Power Systems

12

## REFERENCES

[1] K. G. Boroojeni, M. H. Amini, A. Nejadpak, S. S. Iyengar, B. Hoseinzadeh, and C. L. Bak, "A theoretical bilevel control scheme for power networks with large-scale penetration of distributed renewable resources," in *2016 IEEE International Conference on Electro Information Technology (EIT)*, 2016, pp. 0510–0515.

[2] Department of Energy Office of Electricity Delivery and Energy Reliability. (2012). Summary Report: 2012 DOE Microgrid Workshop.[Online].Available:http://energy.gov/sites/prod/files/2012%20Microgrid%20Workshop%20Report%2009102012.pdf. accessed Nov. 1, 2015.

[3] P. C. Loh, D. Li, Y. K. Chai, and F. Blaabjerg, "Autonomous Control of Interlinking Converter With Energy Storage in Hybrid AC-DC Microgrid," *IEEE Trans. Ind. Appl.*, vol. 49, no. 3, pp. 1374–1382, May 2013.

[4] R. H. Lasseter and P. Paigi, "Microgrid: A conceptual solution," in *Power Electronics Specialists Conference, 2004. PESC 04. 2004 IEEE 35th Annual*, 2004, vol. 6, pp. 4285–4290.

[5] C. Gouveia, J. Moreira, C. L. Moreira, and J. A. P. Lopes, "Coordinating Storage and Demand Response for Microgrid Emergency Operation," *IEEE Trans. Smart Grid*, vol. 4, no. 4, pp. 1898–1908, Dec. 2013.

[6] W. A. Omran, M. Kazerani, and M. M. A. Salama, "Investigation of Methods for Reduction of Power Fluctuations Generated From Large Grid-Connected Photovoltaic Systems," *IEEE Trans. Energy Convers.*, vol. 26, no. 1, pp. 318–327, Mar. 2011.

[7] K. Boroojeni, M. H. Amini, A. Nejadpak, T. Dragicevic, S. S. Iyengar, and F. Blaabjerg, "A Novel Cloud-Based Platform for Implementation of Oblivious Power Routing for Clusters of Microgrids," *IEEE Access*, vol. 5, pp. 607–619, 2017.

[8] A. Khodaei, "Provisional Microgrids," *IEEE Trans. Smart Grid*, vol. 6, no. 3, pp. 1107–1115, May 2015.

[9] S. Gill, E. Barbour, I. A. G. Wilson, and D. Infield, "Maximising revenue for non-firm distributed wind generation with energy storage in an active management scheme," *IET Renew. Power Gener.*, vol. 7, no. 5, pp. 421–430, Sep. 2013.

[10] E. Sortomme and M. A. El-Sharkawi, "Optimal Power Flow for a System of Microgrids with Controllable Loads and Battery Storage," in *2009 IEEE/PES Power Systems Conference and Exposition*, 2009, pp. 1–5.

[11] S. Parhizi, H. Lotfi, A. Khodaei, and S. Bahramirad, "State of the Art in Research on Microgrids: A Review," *IEEE Access*, vol. 3, pp. 890–925, 2015.

[12] J. Eyer and G. Corey, "Energy storage for the electricity grid: Benefits and market potential assessment guide," *Sandia Natl. Lab.*, vol. 20, no. 10, p. 5, 2010.

[13] Q. Fu, A. Hamidi, A. Nasiri, V. Bhavaraju, S. B. Krstic, and P. Theisen, "The Role of Energy Storage in a Microgrid Concept: Examining the opportunities and promise of microgrids.," *IEEE Electrification Mag.*, vol. 1, no. 2, pp. 21–29, Dec. 2013.

[14] M. Koller, T. Borsche, A. Ulbig, and G. Andersson, "Defining a degradation cost function for optimal control of a battery energy storage system," in *PowerTech (POWERTECH), 2013 IEEE Grenoble*, 2013, pp. 1–6.

[15] C. Ju and P. Wang, "Energy management system for microgrids including batteries with degradation costs," in *Power System Technology (POWERCON), 2016 IEEE International Conference on*, 2016, pp. 1–6.

[16] Y. Zhang and M.-Y. Chow, "Microgrid cooperative distributed energy scheduling (CoDES) considering battery degradation cost," in *Industrial Electronics (ISIE), 2016 IEEE 25th International Symposium on*, 2016, pp. 720–725.

[17] K. Abdulla *et al.*, "Optimal Operation of Energy Storage Systems Considering Forecasts and Battery Degradation," *IEEE Trans. Smart Grid*, pp. 1–1, 2016.

[18] E. Hajipour, M. Bozorg, and M. Fotuhi-Firuzabad, "Stochastic Capacity Expansion Planning of Remote Microgrids With Wind Farms and Energy Storage," *IEEE Trans. Sustain. Energy*, vol. 6, no. 2, pp. 491–498, Apr. 2015.

[19] J. P. Fossati, A. Galarza, A. Martín-Villate, and L. Fontán, "A method for optimal sizing energy storage systems for microgrids," *Renew. Energy*, vol. 77, pp. 539–549, May 2015.

[20] A. Toliyat and A. Kwasinski, "Energy storage sizing for effective primary and secondary control of low-inertia microgrids," in *2015 IEEE 6th International Symposium on Power Electronics for Distributed Generation Systems (PEDG)*, 2015, pp. 1–7.

[21] T. Kerdphol, Y. Qudaih, and Y. Mitani, "Battery energy storage system size optimization in microgrid using particle swarm optimization," in *IEEE PES Innovative Smart Grid Technologies, Europe*, 2014, pp. 1–6.

[22] M. R. Aghamohammadi and H. Abdolahinia, "A new approach for optimal sizing of battery energy storage system for primary frequency control of islanded Microgrid," *Int. J. Electr. Power Energy Syst.*, vol. 54, pp. 325–333, Jan. 2014.

[23] S. Bahramirad and H. Daneshi, "Optimal sizing of smart grid storage management system in a microgrid," in *2012 IEEE PES Innovative Smart Grid Technologies (ISGT)*, 2012, pp. 1–7.

[24] S. Bahramirad, W. Reder, and A. Khodaei, "Reliability-Constrained Optimal Sizing of Energy Storage System in a Microgrid," *IEEE Trans. Smart Grid*, vol. 3, no. 4, pp. 2056–2062, Dec. 2012.

[25] M. Ross, R. Hidalgo, C. Abbey, and G. Joós, "Analysis of Energy Storage sizing and technologies," in *2010 IEEE Electric Power and Energy Conference (EPEC)*, 2010, pp. 1–6.

[26] M. Asensio, P. M. de Quevedo, G. Munoz-Delgado, and J. Contreras, "Joint Distribution Network and Renewable Energy Expansion Planning considering Demand Response and Energy Storage ?? Part I: Stochastic Programming Model," *IEEE Trans. Smart Grid*, vol. PP, no. 99, pp. 1–1, 2016.

[27] M. Asensio, P. M. de Quevedo, G. Munoz-Delgado, and J. Contreras, "Joint Distribution Network and Renewable Energy Expansion Planning considering Demand Response and Energy Storage ?? Part II: Numerical Results and considered Metrics," *IEEE Trans. Smart Grid*, vol. PP, no. 99, pp. 1–1, 2016.

[28] T. A. Nguyen, M. L. Crow, and A. C. Elmore, "Optimal Sizing of a Vanadium Redox Battery System for Microgrid Systems," *IEEE Trans. Sustain. Energy*, vol. 6, no. 3, pp. 729–737, Jul. 2015.

[29] X. Luo, J. Wang, M. Dooner, and J. Clarke, "Overview of current development in electrical energy storage technologies and the application potential in power system operation," *Appl. Energy*, vol. 137, pp. 511–536, Jan. 2015.

[30] H. Chen, T. N. Cong, W. Yang, C. Tan, Y. Li, and Y. Ding, "Progress in electrical energy storage system: A critical review," *Prog. Nat. Sci.*, vol. 19, no. 3, pp. 291–312, Mar. 2009.

[31] I. Alsaidan, A. Khodaei, and W. Gao, "Determination of battery energy storage technology and size for standalone microgrids," in *2016 IEEE Power and Energy Society General Meeting (PESGM)*, 2016, pp. 1–5.

[32] X. Tan, Q. Li, and H. Wang, "Advances and trends of energy storage technology in Microgrid," *Int. J. Electr. Power Energy Syst.*, vol. 44, no. 1, pp. 179–191, Jan. 2013.

[33] I. Alsaidan, A. Khodaei, and W. Gao, "Distributed energy storage sizing for microgrid applications," in *2016 IEEE/PES Transmission and Distribution Conference and Exposition (T D)*, 2016, pp. 1–5.

[34] N. L. Diaz, T. Dragičević, J. C. Vasquez, and J. M. Guerrero, "Fuzzy-logic-based gain-scheduling control for state-of-charge balance of distributed energy storage systems for DC microgrids," in *2014 IEEE*

*Applied Power Electronics Conference and Exposition - APEC 2014*, 2014, pp. 2171–2176.

[35] W. Li and G. Joos, "Performance Comparison of Aggregated and Distributed Energy Storage Systems in a Wind Farm For Wind Power Fluctuation Suppression," in *2007 IEEE Power Engineering Society General Meeting*, 2007, pp. 1–6.

[36] J. Cui, K. Li, Y. Sun, Z. Zou, and Y. Ma, "Distributed energy storage system in wind power generation," in *2011 4th International Conference on Electric Utility Deregulation and Restructuring and Power Technologies (DRPT)*, 2011, pp. 1535–1540.

[37] E. Karanasios, M. Ampatzis, P. H. Nguyen, W. L. Kling, and A. van Zwam, "A model for the estimation of the cost of use of Li-Ion batteries in residential storage applications integrated with PV panels," in *2014 49th International Universities Power Engineering Conference (UPEC)*, 2014, pp. 1–6.

[38] A. Bocca, A. Sassone, D. Shin, A. Macii, E. Macii, and M. Poncino, "An equation-based battery cycle life model for various battery chemistries," in *Very Large Scale Integration (VLSI-SoC), 2015 IFIP/IEEE International Conference on*, 2015, pp. 57–62.

[39] H. N. Seiger, "Effect of depth of discharge on cycle life of near-term batteries," presented at the 16th Intersociety Energy Conversion Engineering Conference, 1981, pp. 102–110.

[40] A. F. Burke, "Cycle Life Considerations for Batteries in Electric and Hybrid Vehicles," SAE Technical Paper, Warrendale, PA, SAE Technical Paper 951951, Aug. 1995.

[41] L. H. Thaller, "Expected Cycle Life vs. Depth of Discharge Relationships of Well-Behaved Single Cells and Cell Strings," *J. Electrochem. Soc.*, vol. 130, no. 5, pp. 986–990, 1983.

[42] G. Muñoz-Delgado, J. Contreras, and J. M. Arroyo, "Joint Expansion Planning of Distributed Generation and Distribution Networks," *IEEE Trans. Power Syst.*, vol. 30, no. 5, pp. 2579–2590, Sep. 2015.

[43] S. de la Torre, A. J. Conejo, and J. Contreras, "Transmission Expansion Planning in Electricity Markets," *IEEE Trans. Power Syst.*, vol. 23, no. 1, pp. 238–248, Feb. 2008.

[44] A. Khodaei, M. Shahidehpour, and S. Kamalinia, "Transmission Switching in Expansion Planning," *IEEE Trans. Power Syst.*, vol. 25, no. 3, pp. 1722–1733, Aug. 2010.

[45] A. J. Conejo, Ed., *Decomposition techniques in mathematical programming: engineering and science applications*. Berlin ; New York: Springer, 2006.

[46] LONDON ECONOMICS, 2013. "Estimating the Value of Lost Load". Briefing paper prepared for the Electricity Reliability Council of Texas, Inc. by London Economics International LLC. June 17th 2013.

[47] A. Gabash and P. Li, "Active-Reactive Optimal Power Flow in Distribution Networks With Embedded Generation and Battery Storage," *IEEE Trans. Power Syst.*, vol. 27, no. 4, pp. 2026–2035, Nov. 2012.

[48] A. Gabash and P. Li, "Flexible Optimal Operation of Battery Storage Systems for Energy Supply Networks," *IEEE Trans. Power Syst.*, vol. 28, no. 3, pp. 2788–2797, Aug. 2013.

[49] A. Gabash and P. Li, "Variable reverse power flow-Part I: AR-OPF with reactive power of wind stations," in *Environment and Electrical Engineering (EEEIC), 2015 IEEE 15th International Conference on*, 2015, pp. 21–26.

[50] A. Gabash and P. Li, "Variable reverse power flow-part II: Electricity market model and results," in *Environment and Electrical Engineering (EEEIC), 2015 IEEE 15th International Conference on*, 2015, pp. 27–32.

[51] A. Gabash and P. Li, "Active-reactive optimal power flow for low-voltage networks with photovoltaic distributed generation," in *2012 IEEE International Energy Conference and Exhibition (ENERGYCON)*, 2012, pp. 381–386.

[52] A. Gabash, M. E. Alkal, and P. Li, "Impact of allowed reverse active power flow on planning PVs and BSSs in distribution networks considering demand and EVs growth," *Power Energy Stud. Summit PESS 2013 IEEE Stud. Branch Bielef.*, pp. 11–16, 2013.

[53] A. Khodaei, S. Bahramirad, and M. Shahidehpour, "Microgrid Planning Under Uncertainty," *IEEE Trans. Power Syst.*, vol. 30, no. 5, pp. 2417–2425, Sep. 2015.

[54] A. Thiele, T. Terry, and M. Epelman, "Robust linear optimization with recourse," *Rapp. Tech.*, pp. 4–37, 2009.

[55] "Microgrid at Illinois Institute of Technology." [Online]. Available: http://iitmicrogrid.net/microgrid.aspx. [Accessed: 21-Mar-2015].

[56] "Home | ComEd's Hourly Pricing Program." [Online]. Available: https://hourlypricing.comed.com/. [Accessed: 14-Apr-2015].

[57] [Online]. Available: http://industrial.alpha.com/index.php/products.

[58] [Online]. Available: http://www.cdtechno.com/.

[59] [Online]. Available: http://www.odysseybattery.com/documents/us-ody-tm-001_0411_000.pdf

[60] N. Lu, M. R. Weimar, Y. V. Makarov, and C. Loutan, "An evaluation of the NaS battery storage potential for providing regulation service in California," in *2011 IEEE/PES Power Systems Conference and Exposition*, 2011, pp. 1–9.

**Ibrahim Alsaidan** (S'15) received the B.S degree from Qassim University, Saudi Arabia in 2008, and the M.S. degree from University of Denver in 2012, where he is currently pursuing the Ph.D. degree. His research interests include modeling, sizing, and operating energy storage systems in distribution network.

**Amin Khodaei** (SM'14) received his Ph.D. degree in electrical engineering from the Illinois Institute of Technology, in 2010. He was a visiting faculty (2010–2012) in the Robert W. Galvin Center for Electricity Innovation at IIT. He joined the University of Denver, Denver, CO, USA, in 2013 where he is currently an Associate Professor and Chair of the Electrical and Computer Engineering Department. His research interests include power system operation, planning, computational economics, and smart electricity grids.

**Wenzhong Gao** (SM'03) received the M.S. and Ph.D. degrees in electrical and computer engineering, specializing in electric power engineering, from the Georgia Institute of Technology, Atlanta, GA, USA, in 1999 and 2002, respectively. He is currently with the Department of Electrical and Computer Engineering, University of Denver, Denver, CO, USA. His current research interests include renewable energy and distributed generation, microgrid, smart grid, power system protection, power electronics applications in power systems, power system modeling and simulation, and hybrid electric propulsion systems.

Dr. Gao is an Editor of the IEEE TRANSACTIONS ON SUSTAINABLE ENERGY. He is the General Chair of the 48th North American Power Symposium in 2016 and the IEEE Symposium on Power Electronics and Machines in Wind Applications in 2012.